OSCILLATORY EXTINCTION OF SPHERICAL DIFFUSION FLAMES

C. K. Law, S. W. Yoo, and E. W. Christiansen

Department of Mechanical and Aerospace Engineering
Princeton University, Princeton, NJ 08544

INTRODUCTION

Since extinction has been observed in an oscillatory manner in $Le>1$ premixed flames [1], it is not unreasonable to expect that extinction could occur in an unsteady manner for diffusion flames. Indeed, near-limit oscillations have been observed experimentally under microgravity conditions for both candle flames [2] and droplet flames [3]. Furthermore, the analysis of Cheatham and Matalon [4] on the unsteady behavior of diffusion flames with heat loss, identified an oscillatory regime which could be triggered by either a sufficiently large Lewis number (even without heat loss) or an appreciable heat loss (even for $Le=1$).

In light of these recent understanding, the present investigation aims to provide a well-controlled experiment that can unambiguously demonstrate the oscillation of diffusion flames near both the transport- and radiation-induced limits. That is, since candle and jet flames are stabilized through flame segments that are fundamentally premixed in nature, and since premixed flames are prone to oscillate, there is the possibility that the observed oscillation of these bulk diffusion flames could be triggered and sustained by the oscillation of the premixed flame segments. Concerning the observed oscillatory droplet extinction, it is well-known that gas-phase oscillation in heterogeneous burning can be induced by and is thereby coupled with condensed-phase unsteadiness. Consequently, a convincing experiment on diffusion flame oscillation must exclude any ingredients of premixed flames and other sources that may either oscillate themselves or promote the oscillation of the diffusion flame. The present experiment on burner-generated spherical flames with a constant reactant supply endeavored to accomplish this goal. The results are further compared with those from computational simulation for further understanding and quantification of the flame dynamics and extinction.

SPECIFICATION OF EXPERIMENT AND COMPUTATION

An inverse flame configuration was employed with the oxidizer being ejected from a porous sphere burner ($20\mu m$ pore-diameter, $1.27cm$ sphere diameter) into a low-density fuel environment comprising of He and H_2 at a pressure of $0.096atm$ to effectively minimize buoyancy. Various inert gasses (N_2, CO_2, He) were used to dilute the oxidizer in order to change the Lewis number and radiative properties of the mixture so that both the transport-induced and radiative-induced limit could be achieved. A Xybion IMC-201 intensified multi-spectral video camera with a UV-transmissive lens was adopted for visualization. The excited CO_2 (CO_2*) chemiluminescence was used as a marker for detecting the CO_2-diluted flames, whereas OH* due to transition $^2\Sigma^+ \rightarrow {}^2\Pi$, observable at $305.4nm$, was used for the N_2-diluted flames. The radiometer was placed 14 cm from the center of the burner to detect emission changes in the flame before extinction.

Extinction was triggered by gradually decreasing the H_2 mole fraction in the ambient. Four oxidizer mixtures, hereafter referred to as cases (a), (b), (c) and (d), diluted with different

combinations of CO_2, N_2, and/or He flow rates were selected to modify the transport and radiative properties of the mixture. Table 1 lists their respective mixture composition and mass flow rates.

The spherically symmetric unsteady diffusion flame was simulated using a modified version of the code developed by Ref. [5] where terms representing unsteadiness, radiation, heat loss, and boundary conditions for non-premixed burning were added. The flame was assumed to be optically thin with CO_2, CO, and H_2O as radiating species, with respective emission/absorption coefficients obtained from Ju et al. [6]. The mass flow rate m, the burner temperature T_s (432K), the oxidizer and ambient fuel compositions, and the chamber pressure p were selected to simulate the experiment. The size of the computational domain was selected to be the effective radial distance (24.8cm) from the burner surface to the chamber wall. The boundary condition at the end of the computational domain on temperature was the chamber wall temperature measured in the experiment (T_∞=305K). The H_2/O_2 reaction mechanism used was that of Mueller *et al.* [7]. To simulate the effect of adding CO_2 as diluent, Mueller's mechanism was augmented with 9 additional elementary reactions, describing the oxidation of CO and the formation/consumption of HCO from the moist CO mechanism of Kim *et. al.* [8]. Helium was also added to the mechanism simply by assuming the same third body efficiencies as argon.

EXPERIMENTAL AND COMPUTATIONAL RESULTS

In general, as the ambient H_2 mole fraction was decreased, the flame luminosity became weaker and the flame size increased. Furthermore, the occurrence of flame oscillation in terms of luminosity and flame size was not visually discernable. The experimentally determined ambient H_2 mole fractions at flame extinction are listed in Table 1. Although all cases appeared to extinguish without pulsating visibly in terms of the flame size, the recorded emission data for cases (a) and (b) revealed that the flames pulsate at 2.1 and 2.3Hz, shown in Fig. 1, prior to extinction, as was predicted in Ref [9]. For cases (c) and (d), no oscillation was observed as shown in Fig. 2.

The steady-state response of spherically symmetric diffusion flames was computationally simulated for the experimental cases (a) through (d). In general the maximum flame temperature decreased while its location increased as the ambient fuel concentration was decreased. When the maximum flame temperature and the fuel molar concentration were plotted, a typical extinction flame response curve was obtained. Whether the observed extinction limit is transport-induced, for which T_{max} increases with increasing m, or radiation-induced, for which T_{max} decreases with increasing m, may be determined by perturbing the mass flow rate from the burner, as discussed in Ref. [9]. For the four mixtures investigated here, this interrogation reveals that cases (a) and (b) are at the radiation-induced limit, while cases (c) and (d) are at the transport-induced limit.

The unsteady simulations were carried out in order to determine the stability of the steady-state solutions. To do so, a steady-state temperature profile of the near-limit flames was perturbed and the ensuing transient response was noted. The perturbation either damped out and relaxed back to steady-state or triggered a growing oscillatory response resulting in extinction.

Figure 3 shows the maximum temperature versus time for the oxidizer mixture given in case (a). For the 32.20% H_2, the perturbed flame relaxes back to the steady-state solution. However, when the H_2 mole fraction is reduced to 32.19%, oscillatory instability develops and the flame eventually extinguishes after quite a number of cycles. The oscillation grows even faster for 32.18%. Similar behavior was observed for case (b) except that the onset of oscillation was

28.09%. Figure 4 shows the maximum temperature versus time for cases (c) and (d). For case (c), pulsating extinction was not observed computationally; instead the perturbed flame at an ambient H_2 mole fraction of 8.024% would extinguish without any oscillations. For case (d), pulsating extinction was observed at $H_2 = 7.727\%$, while $H_2 = 7.728\%$ is stable, although only one cycle of oscillation is observed before extinction. This also verifies that increase in *Le* in the oxidizer does make the flame pulsate before extinction.

The experimental and computational results are compared in Table 1. It is seen that for oxidizer mixtures with CO_2 (cases (a) and (b)) the computational results over-predict the H_2 mole fraction at extinction by a substantial amount, while the opposite holds for cases (c) and (d). This is mainly due to the two heat transfer mechanisms that were neglected in the computations: (1) heat loss to the rod support and burner, which would promote extinction at higher H_2 mole fractions, (2) radiation reabsorption, which would strengthen the flame. Hence the CO_2-diluted flames were experimentally observed to extinguish at lower fuel concentrations due to the dominance of reabsorption over heat loss to the support, while for cases (c) and (d), flames were observed to extinguish at higher fuel concentrations. Despite the disagreement on the hydrogen concentration at extinction, the experimentally observed frequencies at the onset of oscillation do agree quite well with the calculations, hence providing at least partial support to the notion that the same mechanism is responsible for both the computationally and experimentally observed oscillations. While pulsating extinction was observed computationally for case (d), pulsations were not observed experimentally. However, close inspection of the computationally observed pulsating extinction reveals that the flame extinguishes after only one cycle of oscillation, and the amplitude of oscillation is about 2K (compared to 10K for cases (a) and (b)), suggesting that these oscillations might prove difficult to be observed experimentally.

ACKNOWLEDGEMENTS

REFERENCES

1. Law, C. K., and Sung, C. J., *Prog. Energy Combust. Sci.* 26, 459-505 (2000).
2. Dietrich, D.L., Ross, H.D., and T'ien, J.S., AIAA 94-0429 (1994).
3. Nayagam, V. and Williams, F.A., *Seventh International Conference on Numerical Combustion*, York, England, (1998).
4. Cheatham, S. and Matalon, M., Proc. *Combust. Inst.* 26:1063-1070 (1996).
5. Kee, R.J., Grcar, J.F., Smooke, M.D., and Miller, J.A., Sandia Report, SAND 85-8240, 1985.
6. Ju, Y., Guo, H., Liu, F., and Maruta, K., *J. Fluid Mech.* 379:165-190 (1999).
7. Mueller, M. A., Kim, T.J., Yetter, R.A., and Dryer, F.L., *Int. J. Chem. Kinet.*, 31: 113-125 (1999).
8. Kim, T. J., Yetter, R. A. and Dryer, F. L., *Proc. Combust. Inst.*, 25: 759-766 (1994).
9. Christiansen, E.W., Tse, S.D., and Law, C.K., AIAA 2001-1084 (2001).

Table 1 Comparison of experimental and numerical results, where Leo is the oxidizer Lewis number and Le_F the fuel Lewis number (*No pulsation observed)

	Case (a)		Case (b)		Case (c)		Case (d)	
	Comp.	Exp.	Comp.	Exp.	Comp.	Exp.	Comp.	Exp.
Mixture Composition	87.15% CO_2 / 12.85% O_2		70.95% CO_2 / 16.20% He / 12.85% O_2		87.15% N2 / 12.85% O_2		70.95% N_2 / 16.20% He / 12.85% O_2	
Mass Flowrate (mg/s)	59		59		39		39	
%H_2 at Extinction	32.19	19.1	28.09	20.3	8.024*	15.9*	7.727	17.0*
Le_F	0.91	1	0.94	0.99	1.08	1.02	1.08	1.014
Le_O	0.82	0.82	1.19	1.19	1.14	1.14	1.47	1.47
Frequency (Hz)	2.3	2.1	2.3	2.3	n/a	n/a	0.1	n/a
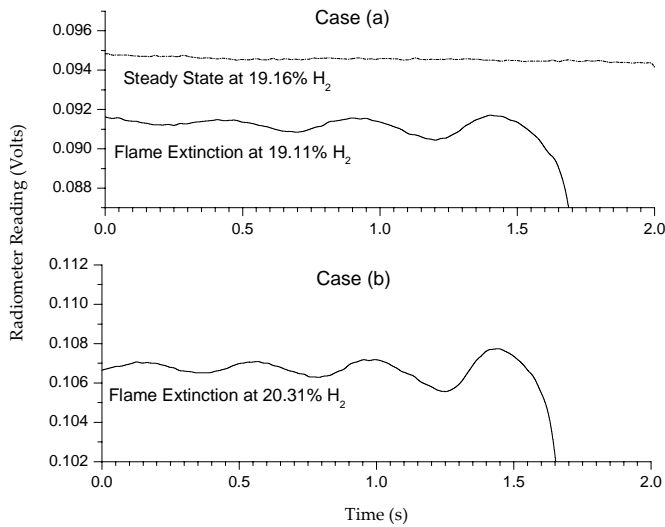
Figure 1 The radiometer voltage readings respect to time near flame extinction for cases (a) and (b). For figure/case (a), steady state flame emission readings are also plotted at hydrogen molar fraction of 19.16%.
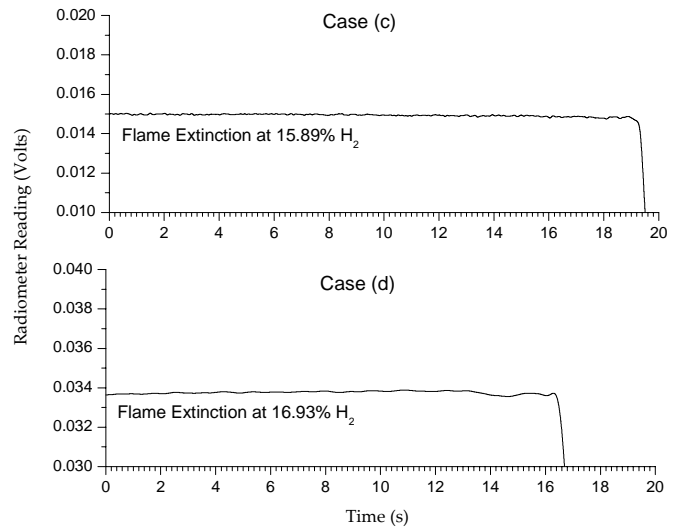
Figure 2 The radiometer voltage readings respect to time near flame extinction for cases (c) and (d).
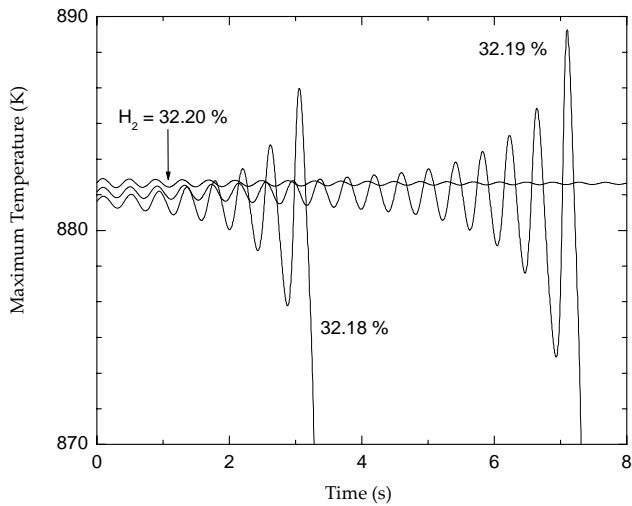
Figure 3 Temporal response of the maximum temperature for case (a), with H_2 = 32.20, 32.19 and 32.18%.
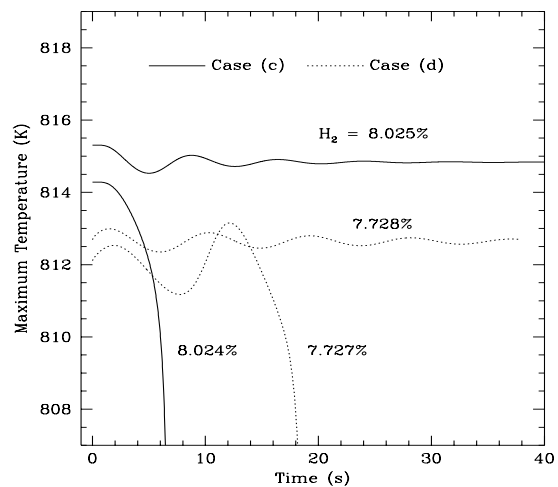
Figure 4 Temporal response of the maximum temperature for case (c), with H_2 = 8.025 and 8.024%, and case (d), with H_2 = 7.728 and 7.727%.